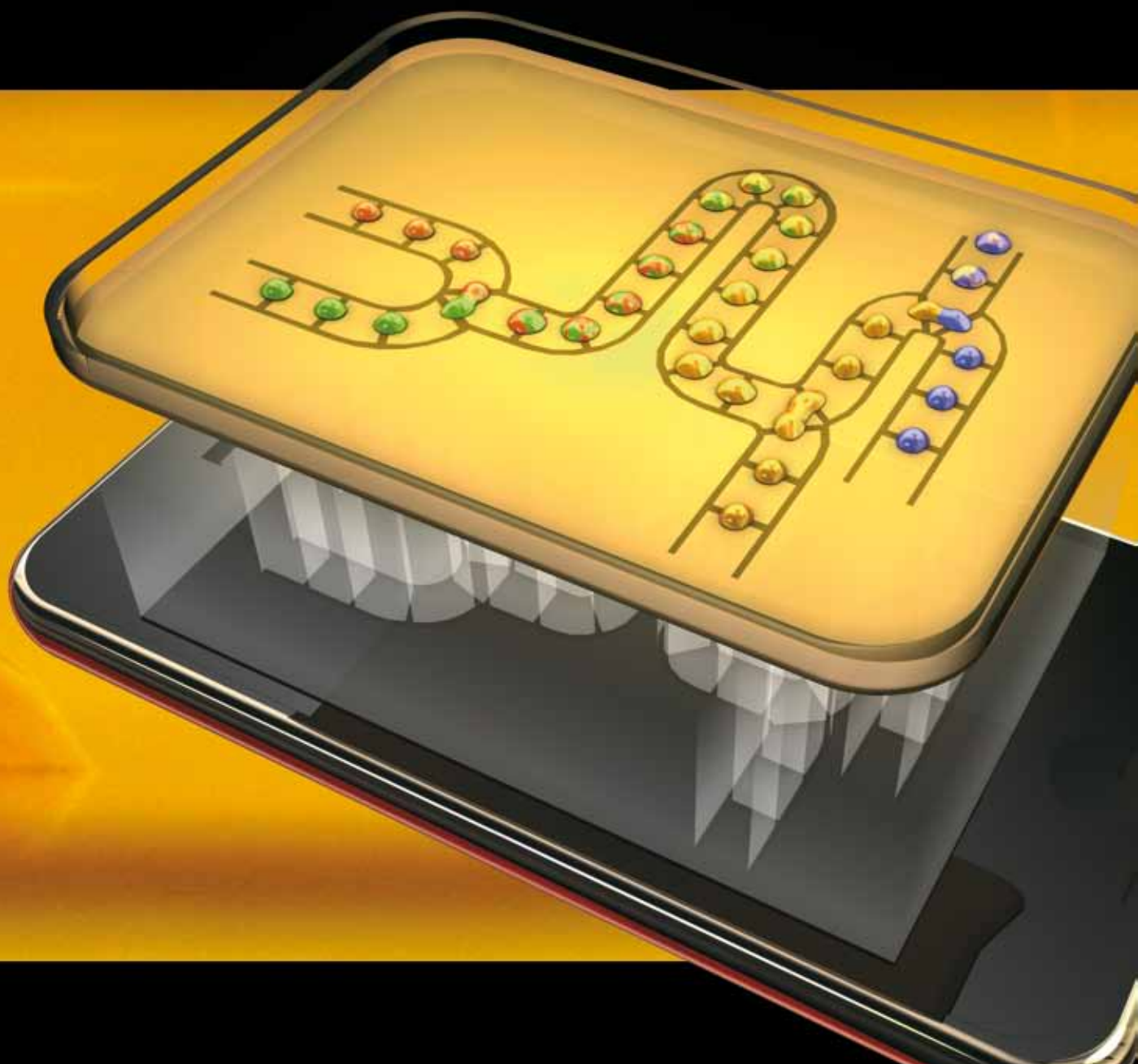


Lab on a Chip

Micro- & nano- fluidic research for chemistry, physics, biology, & bioengineering

www.rsc.org/loc

Volume 10 | Number 13 | 7 July 2010 | Pages 1633–1740



ISSN 1473-0197

RSC Publishing

Chiou
SCOEW for droplet manipulation with
light patterns

Haswell
Rapid PCR amplification

Single-sided continuous optoelectrowetting (SCOEW) for droplet manipulation with light patterns†

Sung-Yong Park,^a Michael A. Teitell^b and Eric P. Y. Chiu^{*a}

Received 20th January 2010, Accepted 13th April 2010

First published as an Advance Article on the web 6th May 2010

DOI: 10.1039/c001324b

Electrowetting-on-dielectric (EWOD) promises to be an important lab-on-a-chip approach for effectively manipulating droplets with electric field-controlled surface tension. Droplets manipulated in electrowetting-based devices are typically sandwiched between two parallel plates and actuated by digital electrodes. The size of pixilated electrodes limits the minimum droplet size that can be manipulated. Here, we report on a single-sided continuous optoelectrowetting (SCOEW) mechanism that enables light-patterned electrowetting modulation for continuous droplet manipulation on an open, featureless, and photoconductive surface. SCOEW overcomes the size limitation of physical pixilated electrodes by utilizing dynamic and reconfigurable optical patterns and enables the continuous transport, splitting, merging, and mixing of droplets with volumes ranging from 50 μL to 250 pL, over 5-orders of magnitude. This single-sided open configuration provides a flexible interface for integration with other microfluidic components, such as sample reservoirs through simple tubing. Light-triggered, parallel, and volume-tunable droplet injection with volume variation less than 1% has been demonstrated with SCOEW. The unique lateral field-driven optoelectrowetting mechanism also enables extremely low light intensity actuation, and droplet manipulation can be achieved by directly positioning the SCOEW chip on a LCD screen used in a laptop or portable cellular phone.

1. Introduction

Droplet-based microfluidic systems have attracted broad interest for lab-on-chip applications. Demonstrated droplet manipulation technologies are versatile and include surface acoustic wave,^{1–4} thermocapillary forces,^{5,6} electrowetting-on-dielectric (EWOD),^{7–11} dielectrophoresis (DEP),^{12–17} and magnetic forces.^{18,19} Among these, EWOD provides advantages in fast response times, easy implementations, and large force at the millimeter to micrometer scales. EWOD-based applications such as polymerase chain reaction (PCR),^{20,21} clinical diagnostics,^{22,23} DNA enrichment and ligation,^{10,24,25} proteomics,^{26,27} electronic paper,²⁸ and on-chip cooling^{29,30} have been shown.

Conventional EWOD devices are typically implemented by sandwiching droplets between two parallel plates and actuation is achieved by addressing digital electrodes.^{7,8,11,20,29,31,32} Droplet manipulation functions such as injection, splitting,

transportation, and merging have been demonstrated on this sandwiched configuration. On the other hand, single-sided EWOD devices, in which both actuating and ground electrodes are integrated on the same substrate, have been demonstrated and showed advantages in manipulating larger droplet volumes per sample footprint, better droplet mixing efficiencies, and flexible integration with other components such as optical detectors and external sample reservoirs.^{10,33–36}

Recently, Chiu *et al.* reported an optoelectrowetting (OEW) mechanism^{37,38} that enables two-dimensional (2D) optical manipulation of droplets and showed droplet-based functions such as injection, transportation, and separation. By using light beams, OEW solved the complex wiring and interconnecting issues faced by EWOD devices using physical metal electrodes when addressing a large number of droplets in parallel on a 2D surface. To overcome the size limitation of pixilated electrodes in both EWOD and OEW devices, Chiu *et al.* also demonstrated a continuous optoelectrowetting (COEW) mechanism that enables continuous transportation of picoliter droplets sandwiched between two featureless and closely positioned electrodes (15 μm separation gap), one transparent ITO electrode and one photoconductive amorphous silicon electrode.³⁹ However, the thick amorphous silicon layer used in COEW for matching the electrical impedance of the dielectric layer is difficult to reproduce due to large residual stress during the deposition process. The large voltage leak in the areas not covered by droplets also causes droplet instability issues and satellite droplets ejected from mother droplets are often observed during experiments. Chuang *et al.* demonstrated an open OEW mechanism⁴⁰ for droplet actuation on a single-sided configuration with pixilated electrodes.

^aDepartment of Mechanical and Aerospace Engineering, University of California at Los Angeles (UCLA), 43-147 Eng. IV, 420 Westwood Plaza, Los Angeles, CA, 90095-1597, USA. E-mail: pychiou@seas.ucla.edu; Fax: +1-310-206-4830; Tel: +1-310-825-8620

^bDepartments of Pathology and Pediatrics, California NanoSystems Institute, Broad Stem Cell Research Center, and Molecular Biology Institute, UCLA, 4-762 MRL, 675 Charles Young Drive South, Los Angeles, CA, 90095-1732, USA. E-mail: MTeitell@mednet.ucla.edu; Fax: +1-310-267-0382; Tel: +1-310-206-6754

† Electronic supplementary information (ESI) available: Five video clips showing (1) continuous light-actuated droplet transportation, (2) light-triggered droplet splitting, (3) droplet merging and mixing, (4) continuous light-triggered droplet injection from an external reservoir, and (5) droplet transportation on a LCD display. See DOI: 10.1039/c001324b

Here, we demonstrate a single-sided continuous optoelectrowetting mechanism (SCOEW) to enable continuous light-patterned electrowetting on a featureless photoconductive surface. It provides several advantages over conventional EWOD and OEW devices, including (1) a single-sided open chamber configuration allows easy integration with other microfluidic components such as sample reservoirs; (2) a continuous photoconductive surface enables droplets to be continuously positioned at any location on a 2D surface; (3) the droplet size limitation determined by the size of physical pixilated electrodes is completely eliminated; (4) compared to any previously demonstrated OEW devices, the lateral field-driven optoelectrowetting mechanism can be operated with extremely low light intensity such as a LCD display without any extra optical components such as lenses.

Our study presents the working principle of SCOEW, numerical simulation results, and demonstrates experimental results including continuous droplet transportation, splitting, merging, mixing, and light-triggered, volume-controlled droplet injection from external reservoirs.

2. SCOEW device structure and light-actuation principle

Fig. 1 illustrates the SCOEW device structure and its equivalent circuit model. The device consists of a glass substrate coated with a 0.5 μm thick featureless hydrogenated amorphous silicon (a-Si:H) layer. Two 0.1 μm thick strip aluminium (Al) electrodes separated by a 5 cm gap are deposited at two ends of this device, and a dc bias is applied to the two aluminium electrodes to provide a lateral electric field across the entire SCOEW device. A 1 μm thick amorphous fluorocarbon polymer, Cytop (CTL-809M), is spin-coated on the a-Si:H surface to provide a hydrophobic dielectric layer. Aqueous droplets are positioned on top of the hydrophobic Cytop surface and immersed in oil. Dynamic optical image patterns are generated by a commercial projector and focused on the amorphous silicon layer.

Droplet actuation on SCOEW is achieved by creating a contact angle difference between the two edges of a droplet

using specifically configured light patterns. According to the Young–Lippmann equation,⁹ the contact angle of a droplet is determined by the local voltage drop across the dielectric layer between the droplet and the underlying electrodes:

$$\cos\theta = \cos\theta_0 + \frac{1}{2\gamma} cV^2 \quad (1)$$

where c is the specific capacitance, γ is the surface tension between the droplet and surrounding medium, and V is the voltage drop across a dielectric layer in the vertical direction at the three-phase contact line. In SCOEW, θ_0 and θ represent the droplet contact angle before and after the illumination of a specific light pattern.

The principle of droplet actuation on a SCOEW surface can be qualitatively explained by a simplified equivalent circuit model, as in Fig. 1. The a-Si:H layer is modeled as serially connected photoresistors. The dielectric layer between a droplet and an a-Si:H layer is modeled as capacitors forming a shunt circuit. The water resistance can be neglected under the application of a dc bias due to its low electrical impedance compared to the capacitors. Without light illumination or under uniform light illumination, the voltage linearly drops across the entire device in the a-Si:H layer. As a result, the voltage drop from b to e is equally divided by the two capacitors, $V_{bc} = V_{de} = 1/2V_{be}$. This implies that the contact angles at the two edges of a droplet are equal in cases with no light illumination or under uniform illumination. If two light beams with equal intensity illuminate the two photoresistors outside the droplet to decrease their resistances, the voltage V_{bc} will increase and cause the contact angle to decrease at the two edges of the droplet. If all photoresistors, except the one underneath the droplet, are illuminated, then $V_{bc} \neq V_{de}$ due to this asymmetrical illumination. This creates a contact angle difference at the two droplet edges and a net surface tension force is created to move the droplet toward the non-illuminated site.

Compared to prior optically-actuated electrowetting devices, there is an important and unique feature in SCOEW actuation. The dielectric capacitors and the photoresistors form a shunt-equivalent circuit. The electrowetting voltage across the two capacitors is determined by the relative ratio of photoresistances between photoresistors and not their absolute values. A 2-fold photoconductivity difference between the illuminated and non-illuminated sites is sufficient to induce a significant electrowetting voltage difference to actuate a droplet. This unique property allows optical actuation of droplets on a SCOEW device with low optical intensity for large area manipulations.

3. Numerical simulation results

Analysis using an equivalent circuit model provides a qualitative explanation of the electrowetting effect in SCOEW. To better understand the electrowetting voltage drop along the three phase contact line of a droplet, a 3D finite element model was constructed using COMSOL Multiphysics 3.2 to simulate the electric field distribution. Since the droplet size used in experiments ranges from hundreds of picoliters to tens of microliters, the diameter of a droplet is much larger than the thickness of the dielectric and the photoconductive layers. Simulations using real dimensions take long computation times. To simplify, a 10- μm Cytop, a 5 μm a-Si:H, and a 550 μm thick electrically-insulating

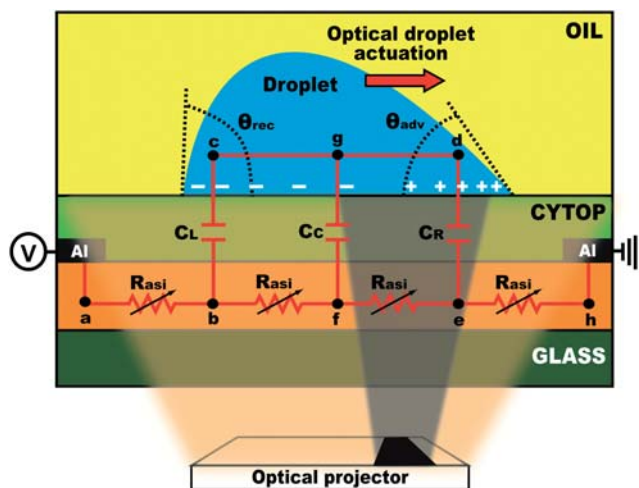


Fig. 1 Schematic of the SCOEW working principle and its equivalent circuit model.

oil layer are used for simulations. A 100 V dc bias is applied at the two end planes separated by a 1 mm gap to create a lateral electric field along the x-direction. The dark conductivity and the photoconductivity in the a-Si:H layer is assumed to be 10^{-8} S/m and 2×10^{-8} S/m, only a 2-fold difference.

Three different cases are compared and shown in Fig. 2. In case (a), the droplet sitting on a hydrophobic surface has a contact angle larger than 90° . A dark bar pattern whose width is as wide as the droplet contact area symmetrically illuminates the center of the droplet. The voltage distribution profiles on the top and the bottom surfaces of the dielectric layer were extracted from the simulation results and plotted. The voltage differences (V_{bc} and V_{de}) between these two surfaces are responsible for the electrowetting effect. In case (a), V_{bc} is equal to V_{de} , which means the droplet contact angles at the two edges decrease by the same amount, causing the droplet to spread out symmetrically along the x direction. In case (b), the width of the dark bar pattern increases to match the width of the spreading droplet. The illumination of a wider dark bar increases the value of V_{bc} and V_{de} , which causes the droplet to spread out further. In case (c), a dark bar pattern illuminates only one side of the droplet. This nonsymmetrical illumination causes a difference in the

electrowetting voltage, $V_{bc} \neq V_{de}$, at the two edges of a droplet, which results in a net surface tension force that moves the droplet toward the dark bar.

4. Experimental results

Continuous, light-pattern controlled contact angle modulation

One interesting feature of SCOEW is that the droplet contact angle can be continuously modulated by optical patterns without changing the applied voltage. Fig. 3 demonstrates the continuous contact angle modulation of a $5 \mu\text{L}$ water droplet immersed in oil and positioned on top of the hydrophobic Cytop layer in SCOEW. Without light illumination or under uniform light illumination, the shape of the droplet remains spherical even under the application of a lateral dc voltage (Fig. 3(a),(b)). When a dark bar pattern is projected in the middle of the droplet, the contact angle decreases (Fig. 3(c)). With the increasing width of the projected dark pattern, the contact angle keeps decreasing and the droplet is stretched along the lateral electric field direction and reaches a contact angle of 60° , as shown in Fig. 3(d).

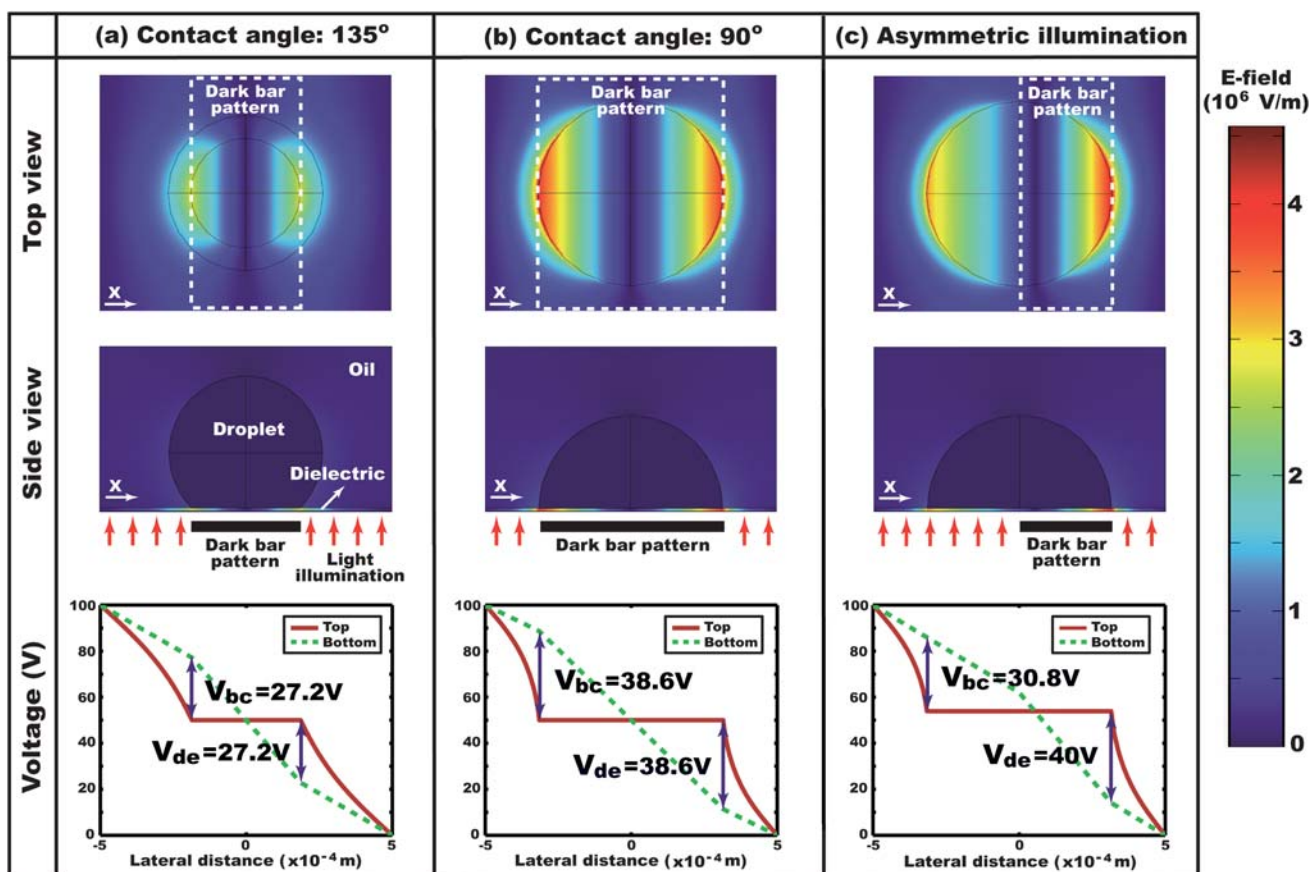


Fig. 2 Simulations of the electric field around a droplet under the illumination of various dark bar patterns are shown in the first two rows. The last row shows the voltage distribution profiles extracted from the top and the bottom surfaces of the dielectric layer. The voltage drops (V_{bc} and V_{de}) between these two surfaces are responsible for actuating the electrowetting effect at the two edges of a droplet. Three different situations are considered. In case (a), a droplet with an initial contact angle larger than 90° is illuminated by a dark bar pattern whose width is as wide as the contact area. In case (b), the droplet in case (a) spreads out to have a contact angle of 90° and is illuminated by a wider dark bar pattern. In case (c), a dark bar pattern only illuminates the right-hand side of the droplet.

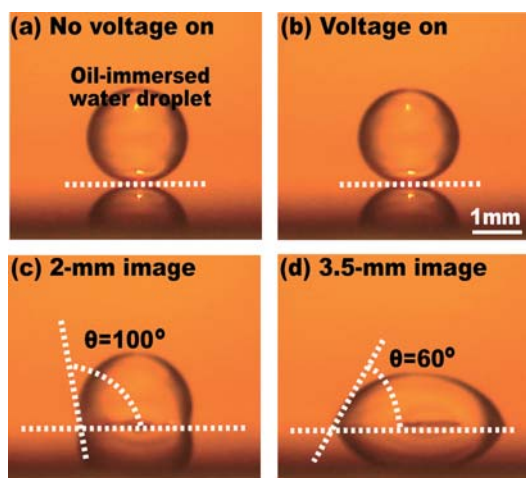


Fig. 3 Video snapshots showing the continuous contact angle modulation of a 5 μL water droplet by varying the width of the projected dark bar pattern. (a) No voltage application. (b) A dc bias is laterally applied between the two Al electrodes but no pattern illuminates. The droplet remains spherical. When a dark bar pattern is projected in the middle of the droplet, the droplet contact angle gradually decreases as the width of the pattern slowly increases. (c) and (d) show the contact angles with the width of the dark bar at 2 mm and 3.5 mm, respectively.

Continuous light-actuated droplet transportation

Continuous droplet transport can be achieved in SCOEW due to its featureless photoconductive layer. Droplets can be continuously addressed to any arbitrary location on a 2D surface. This property also overcomes the size limitation of pixelated electrodes in conventional EWOD and OEW devices and enables transportation of small droplets. Fig. 4(a) demonstrates the transportation of a 50 μL water droplet at a speed of 17.5 mm/s using a 3.5 mm wide moving dark bar pattern (see movie 1, ESI†). By reducing the dark bar width to 100 μm , we have also achieved the transportation of a 250 pL green-colored dye droplet (diameter $\sim 80 \mu\text{m}$) at a speed of 102 $\mu\text{m/s}$ (Fig. 4(b)). These examples show that droplets with a wide range of volume, from tens of microliters to hundreds of picoliters, can be manipulated by simply programming the projected light pattern.

Light-triggered droplet splitting

Compared to droplet transportation, droplet splitting and injection from reservoirs are more challenging processes for

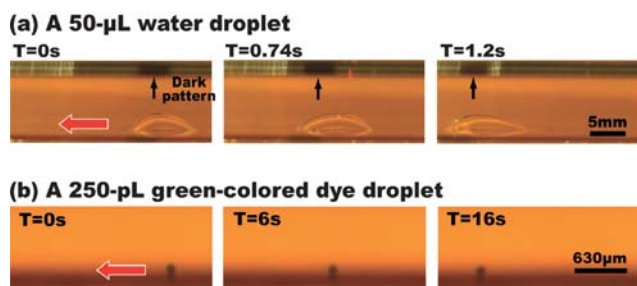


Fig. 4 Video snapshots showing the continuous transportation of (a) 50 μL water and (b) 250 pL green-colored dye droplets by moving various dark bar patterns.

electrowetting devices. To successfully achieve the droplet splitting process in conventional EWOD devices, Cho *et al.* has reported that small gap spacing between the top and bottom electrodes is required to provide a constraint on the droplet height, which also limits the droplet volume that can be manipulated.⁸ The smaller the droplet, the smaller the allowed gap size. In both single-sided EWOD and OEW devices with an open configuration, droplet splitting is more difficult and has not been experimentally demonstrated.^{33,35,40–42}

Here, we demonstrate light-triggered droplet splitting on an open SCOEW device. Fig. 5 demonstrates the splitting of 1 μL and 20 nL droplets by projecting a 6 mm wide and a 4 mm wide dark bar pattern, respectively (see movie 2, ESI†). The droplet initially sits on top of the SCOEW surface. Under a sudden illumination by a dark bar pattern, the droplet is stretched and split into two. An interesting phenomenon that has been observed during experiments is that the droplet splits only when a wide enough dark bar pattern is suddenly applied. The droplet does not split if a narrow dark bar is projected and then followed by gradually increasing the width of the dark bar. This result implies that inertia forces might play a critical role in the droplet splitting process in SCOEW. More studies on the droplet splitting process are required to determine the forces involved during this dynamic process.

Droplet merging and mixing

Droplet merging and mixing are two important droplet manipulation functions. Fig. 6 demonstrates droplet merging and mixing functions using SCOEW (see movie 3, ESI†). Two droplets, one 2 μL water and one 0.5 μL water with a dissolved green dye, are brought close to each other. Since aqueous droplets in oil medium also induce electrical dipoles, the electrostatic dipole–dipole interaction force between two closely

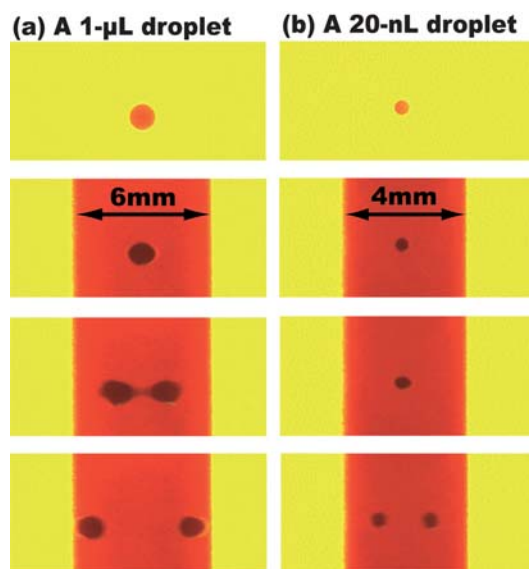


Fig. 5 Video snapshots showing (a) 1 μL green dye droplet splitting by illuminating a 6 mm wide dark bar pattern, and (b) 20 nL green dye droplet splitting using a 4 mm wide dark pattern in SCOEW. Each snapshot has a 0.13 s time delay.

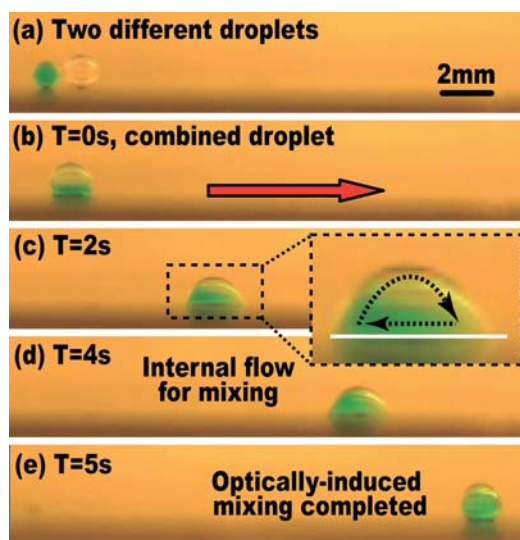


Fig. 6 Two droplets (2 μL and 0.5 μL) are merged and mixed in a SCOEW device. Mixing is accomplished by transporting the merged droplet along a zigzag path on a SCOEW surface.

positioned droplets causes electrocoalescence and merges them into one.^{43,44} To mix the content inside the combined droplet, the droplet is transported along a zigzag path on a SCOEW surface. During transportation, the shear force from the bottom surface enhances internal flows inside the droplet and results in droplet mixing as shown in Fig. 6(e).

Light-triggered droplet dispensing from external reservoirs

The open configuration of SCOEW allows flexible integration with other microfluidic components such as sample reservoirs. Fig. 7(a) illustrates how dynamic optical patterns can be programmed to trigger droplet injection from an external sample reservoir into a SCOEW device. The sample reservoir is located at a position higher than the SCOEW device to provide a constant hydrostatic pressure that delivers liquid down into the

oil chamber through a pin connector. The tip of the pin is located at 2 mm above the SCOEW surface. A dynamic 1D dark bar conveyor moving from left to right at a constant speed of 1 mm/s is projected. During the injection process, the size of the droplet at the tip gradually grows. When the droplet is large enough to touch the SCOEW surface, the dark bar pattern induces the electrowetting effect to pinch off the droplet from the tip and carry it to the right. Fig. 7(b) shows snapshots of this light-triggered droplet injection process (see movie 4, ESI†). In this example, 2.5 μL droplets are continuously injected at a speed of 7 droplets/min into a SCOEW device and transported away.

Precise volume control of injected droplets is very important in many lab-on-chip applications for quantitative analyses. The volume variation of light-triggered and injected droplets in SCOEW was analyzed by taking the cross section images of injected droplets under no external dc voltage, in which all injected droplets return to their spherical shape for easy comparisons. Using an image processing toolbox in MATLAB 7.1, color-scale droplet images are converted into digital black and white images. By counting the number of pixels enclosed by the boundaries as indicated in Fig. 7(c), the volume variation of injected droplets can be estimated. For the example shown in Fig. 7(c), the cross sectional area of 4 injected droplets was counted and was 1567 ± 15 pixels (0.957% area variation), which corresponds to a 0.91% volume variation.

Parallel and volume-tunable droplet injection from multiple reservoirs has also been accomplished by simply connecting multiple pins into the SCOEW oil chamber. Fig. 8 shows an example of droplet injection from two different reservoirs using optical conveyors moving at the same speed but with different periodicities. In the top conveyor, 1.8 μL droplets are dispensed, whereas in the bottom conveyor, whose dark bar periodicity is 2-fold shorter, the volume of the injected droplets is 0.9 μL .

Droplet actuation on a LCD display

The low light intensity requirement of the lateral field-driven optoelectrowetting mechanism enables SCOEW to be operated

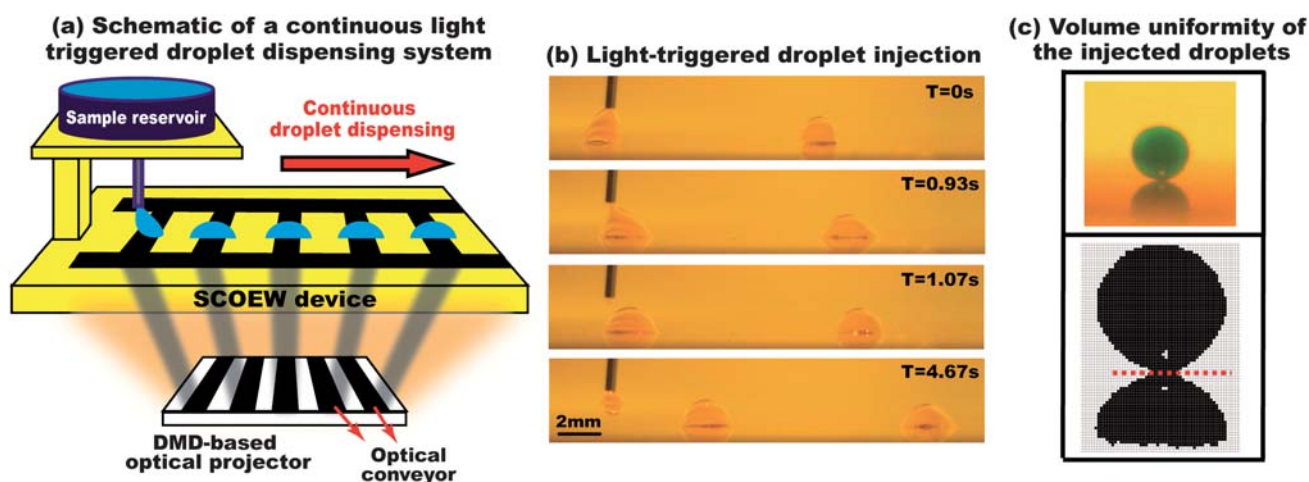


Fig. 7 (a) Schematic showing SCOEW integration with an external sample reservoir through a pin connector for light-triggered droplet injection. (b) Video snapshots demonstrating 2.5 μL droplets are continuously injected into a SCOEW chamber. (c) This injection process is highly reproducible. The volume variation of injected droplets is less than 1%, proved by the four droplets injected at different time frames.

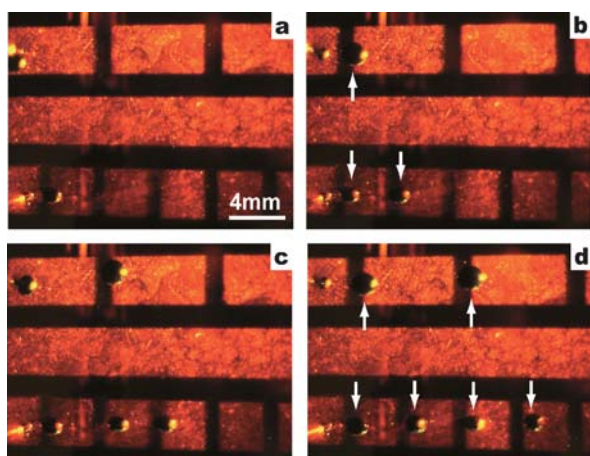


Fig. 8 Parallel light-triggered droplet injection from two external reservoirs. Droplets with volumes of 1.8 μL (top conveyer) and 0.9 μL droplets (bottom) are continuously injected and transported away by two dark bar conveyers with different periodicities. Each snapshot has a 12.94 s time delay.



Fig. 9 Optical actuation of a droplet in a SCOEW device directly positioned on top of the LCD display of a personal computer.

by simply positioning the chip on a LCD display without any extra optical components such as lenses for focusing images. Fig. 9 shows that a 0.5 μL water droplet is transported by a 1.3 mm wide dark pattern at a speed of 510 $\mu\text{m/s}$ (see movie 5, ESI†). This unique feature promises a compact, and portable SCOEW system for massively parallel droplet manipulation.

5. Conclusions

We report a novel single-sided continuous optoelectrowetting (SCOEW) mechanism that enables continuous optical modulation of the electrowetting effect on a single-sided, featureless, and photoconductive surface. SCOEW provides several unique features and advantages over conventional EWOD and OEW devices, including (1) continuous positioning of droplets at any location on a 2D surface; (2) transporting small droplets without the size limitation determined by the physical electrode size; (3) low fabrication cost due to its featureless device structure; (4) an open chamber configuration that allows easy integration with other microfluidic components such as sample reservoirs; and (5) low-light intensity requirement for droplet actuation due to the lateral field-driven optical electrowetting modulation.

With optical patterns from a commercially-available optical projector, we have demonstrated various droplet manipulation functions, including droplet transporting with volumes ranging from 50 μL to 250 pL, droplet splitting, volume-tunable parallel droplet injection from multiple reservoirs with volume variations

less than 1%, and droplet merging and mixing. Droplet manipulation has also been achieved by low-intensity light sources such as a LCD display. SCOEW promises to deliver a large-scale droplet manipulation platform for parallel droplet processing on a low cost substrate using a highly scalable, reconfigurable, and flexible optical addressing method.

Acknowledgements

This project is supported by a NSF CAREER Award (ECCS-0747950), NSF grants (ECCS-0901154 and CBET 0853500), and the NIH Roadmap for Medical Research Nanomedicine Initiative (PN2EY018228).

References

- 1 D. Beyssen, L. L. Brizoual, O. Elmazria and P. Alnot, *Sens. Actuators, B*, 2006, **118**, 380–385.
- 2 Z. Guttenberg, H. Müller, H. Habermüller, A. Geisbauer, J. Pipper, J. Felbel, M. Kielpinski, J. Scriba and A. Wixforth, *Lab Chip*, 2005, **5**, 308–317.
- 3 J. Shi, D. Ahmed, X. Mao, S.-C. S. Lin, A. Lawit and T. J. Huang, *Lab Chip*, 2009, **9**, 2890–2895.
- 4 T. Franke, A. R. Abate, D. A. Weitz and A. Wixforth, *Lab Chip*, 2009, **9**, 2625–2627.
- 5 J. Z. Chen, S. M. Troian, A. A. Darhuber and S. Wagner, *J. Appl. Phys.*, 2005, **97**, 014906.
- 6 A. T. Ohta, A. Jamshidi, J. K. Valley, H.-Y. Hsu and M. C. Wu, *Appl. Phys. Lett.*, 2007, **91**, 07413.
- 7 D. Brassardab, L. Malicac, F. Normandina, M. Tabrizianc and T. Veres, *Lab Chip*, 2008, **8**, 1342–1349.
- 8 S. K. Cho, H. Moon and C.-J. Kim, *J. MEMS*, 2003, **12**, 70–80.
- 9 M. Vallet, B. Berge and L. Vovelle, *Polymer*, 1996, **37**, 2465–2470.
- 10 M. Abdelgawad, S. L. S. Freire, H. Yang and A. R. Wheeler, *Lab Chip*, 2008, **8**, 672–677.
- 11 J. Gong and C.-J. Kim, *Lab Chip*, 2008, **8**, 898–906.
- 12 S.-Y. Park, C. Pan, T.-H. Wu, C. Kloss, S. Kalim, C. E. Callahan, M. Teitell and E. P. Y. Chiou, *Appl. Phys. Lett.*, 2008, **92**, 151101.
- 13 J. A. Schwartz, J. V. Vykoukal and P. R. C. Gascoyne, *Lab Chip*, 2004, **4**, 11–17.
- 14 S.-Y. Park, S. Kalim, C. Callahan, M. A. Teitell and E. P. Y. Chiou, *Lab Chip*, 2009, **9**, 3228–3235.
- 15 K. Ahn, C. Kerbage, T. P. Hunt, R. M. Westervelt, D. R. Link and D. A. Weitz, *Appl. Phys. Lett.*, 2006, **88**, 024104.
- 16 O. D. Velev, B. G. Prevo and K. H. Bhatt, *Nature*, 2003, **426**, 515–516.
- 17 J.-C. Baret, O. J. Miller, V. Taly, M. Ryckelynck, A. El-Harrak, L. Frenz, C. Rick, M. L. Samuels, J. B. Hutchison, J. J. Agresti, D. R. Link, D. A. Weitz and A. D. Griffiths, *Lab Chip*, 2009, **9**, 1850–1858.
- 18 Z.-G. Guo, F. Zhou, J.-C. Hao, Y.-M. Liang, W. T. S. Huck and W.-M. Liu, *Appl. Phys. Lett.*, 2006, **89**, 081911.
- 19 M. Okochi, H. Tsuchiya, F. Kumazawa, M. Shikida and H. Honda, *J. Biosci. Bioeng.*, 2010, **109**, 193–197.
- 20 Y.-H. Chang, G.-B. Lee, F.-C. Huang, Y.-Y. Chen and J.-L. Lin, *Biomed. Microdevices*, 2006, **8**, 215–225.
- 21 K. Ugsornrat, T. Maturus, A. Jomphoak, T. Pogfai, N. V. Afzulpurkar, A. Wisitsoraat and A. Tuantranont, *13th Int. Conf. on Biomed. Eng.*, 2008, **23**, 859–862.
- 22 V. Srinivasan, V. K. Pamula and R. B. Fair, *Lab Chip*, 2004, **4**, 310–315.
- 23 V. Srinivasan, V. K. Pamula and R. B. Fair, *Anal. Chim. Acta*, 2004, **507**, 145–150.
- 24 Y.-J. Liu, D.-J. Yao, H.-C. Lin, W.-Y. Chang and H.-Y. Chang, *J. Micromech. Microeng.*, 2008, **18**.
- 25 H.-C. Lin, Y.-J. Liu and D.-J. Yao, *4th IEEE Int. Conf. on Nanol. Micro Engineered and Molecular Syst.*, 2009, 385–389.
- 26 A. R. Wheeler, H. Moon, C. A. Bird, R. R. O. Loo, C.-J. Kim, J. A. Loo and R. L. Garrell, *Anal. Chem.*, 2005, **77**.
- 27 H. Moon, A. R. Wheeler, R. L. Garrell, J. A. Loo and C.-J. Kim, *Lab Chip*, 2006, **6**, 1213–1219.
- 28 R. A. Hayes and B. J. Feenstra, *Nature*, 2003, **425**, 383–385.

-
- 29 P. Y. Paik, V. K. Pamula and K. Chakrabarty, *IEEE Trans. Very Large Scale Integration (VLSI) Syst.*, 2008, **16**.
- 30 E. Baird and K. Mohseni, *IEEE Trans. Components and Packaging Technologies*, 2008, **31**.
- 31 M. G. Pollack, R. B. Fair and A. D. Shenderov, *Appl. Phys. Lett.*, 2000, **77**.
- 32 G. J. Shah, A. T. Ohta, E. P.-Y. Chiou, M. C. Wu and C.-J. Kim, *Lab Chip*, 2009, **9**, 1732–1739.
- 33 C. G. Cooney, C.-Y. Chen, M. R. Emerling, A. Nadim and J. D. Sterling, *Microfluid. Nanofluid.*, 2006, **2**, 435–446.
- 34 M. Abdelgawad and A. R. Wheeler, *Adv. Mater.*, 2007, **19**, 133–137.
- 35 U.-C. Yi and C.-J. Kim, *J. Micromech. Microeng.*, 2006, **16**, 2053–2059.
- 36 Y. Fouillet and J. L. Achard, *C. R. Phys.*, 2004, **5**.
- 37 P. Y. Chiou, H. Moon, H. Toshiyoshi, C. J. Kim and M. C. Wu, *Sens. Actuators, A*, 2003, 22–228.
- 38 P.-Y. Chiou, Z. Chang and M. C. Wu, *J. MEMS*, 2008, **17**, 133–138.
- 39 P. Y. Chiou, S.-Y. Park and M. Wu, *Appl. Phys. Lett.*, 2008, **93**, 221110.
- 40 H.-S. Chuang, A. Kumar and S. T. Wereley, *Appl. Phys. Lett.*, 2008, 93.
- 41 A. R. Wheeler, *Science*, 2008, **322**, 539–540.
- 42 N. A. Mousa, M. J. Jebrail, H. Yang, M. Abdelgawad, P. Metalnikov, J. Chen, A. R. Wheeler and R. F. Casper, *Sci. Transl. Med.*, 2009, **1**, 1ra2.
- 43 C. Priest, S. Herminghaus and R. Seemann, *Appl. Phys. Lett.*, 2006, **89**, 134101.
- 44 J. S. Eow and M. Ghadiri, *Colloids Surf., A*, 2003, **219**, 253–279.